Photoelectric Emission from Silicon for Photon Energies of 6 to 9.6 eV

T. A. CALLCOTT
Bell Telephone Laboratories, Murray Hill, New Jersey
(Received 26 April 1967)

Energy distributions of photoemitted electrons from cleaved (111) silicon surfaces are given for photon energies from 6 to 9.6 eV. Distributions from clean surfaces and from such surfaces covered with up to a monolayer of cesium are given. A full monolayer deposition of cesium is found to move the surface Fermi level ≤ 0.4 eV above its clean surface position 0.33 eV above the valence-band edge (E_v). Structure in the distributions at energy positions $\lesssim E_v+4.3$ eV is nearly stationary in energy with changing photon energy. The contribution of secondaries to a peak at $E_v+2.8$ eV is clearly evident. A dip is found in the distributions at $\sim E_v+3.1$ eV which lends strong support to the proposal that transport effects can strongly modify the initially excited internal energy distribution. Structure appearing at energies $\gtrsim E_v+4.5$ eV is found to move in energy position more slowly than the change in photon energy. This behavior indicates that the structure is associated with direct optical transitions.

I. INTRODUCTION

SEVERAL authors have reported photoemission measurements on clean silicon surfaces.[1–7] Most extensive work has been done by Gobeli and Allen, who have measured spectral yield and energy distributions of photoelectrons for photon energies $3 \leq h\nu \leq 6.2$ eV. Most of these measurements were made on uniquely good cleaved silicon surfaces, and on such surfaces covered with up to a monolayer of cesium, applied to lower the work function.

In theoretical analyses of optical and photoemission effects in silicon, it has usually been assumed that the bulk of optical transitions are direct.[8–10] This assumption gives a good account of the spectral yield and optical reflectivity in the photon-energy range below 6 eV [1,8] and draws support from measurements of the yield near the photoemission threshold[3] and the angular distribution of photoemitted electrons.[5] To account for the shape of the energy distributions of emitted electrons with this assumption, however, Kane found it necessary to invoke transport effects that modify the initial internal distribution as the electrons move to the surface.[11] Spicer and Eden have contended, on the other hand, that a combination of direct and "nondirect" transitions gives a better fit to both the yield and energy distribution data in the photon energy range below 6 eV and have suggested that nondirect transitions become increasingly important at higher energies.[12] A similar conclusion is suggested by an analysis of silicon optical data by Ehrenreich and Phillip, indicating that direct transitions are of little importance in the photon-energy range from 8 to 16 eV.[13]

This paper reports measurements of energy distributions of photoemitted electrons excited by photons of energy $6 < h\nu \leq 9.6$ eV. Distributions from clean-cleaved (111) silicon surfaces and from such surfaces covered with partial and full monolayers of cesium are presented and discussed. The data indicate that structure in the distributions resulting from photoexcitation to final states more than ~ 4.3 eV above the valence-band edge can best be attributed to direct transitions without, however, ruling out the possibility that indirect transitions contribute a background to that structure. At lower energies the results are less conclusive, but do exhibit a clear feature which we attribute to a major transport effect proposed by Kane. New information is also obtained on the position of the Fermi level at a cesium-covered silicon surface.

II. RESUMÉ OF CONCEPTS AND PREVIOUS RESULTS

The interpretation of the present work is greatly influenced by the earlier measurements of Gobeli and Allen, and by the theoretical calculations of E. Kane. A summary of pertinent results of their work is given below along with a brief discussion of the concepts necessary for interpreting photoemission data. The results are usually stated without justification other than a reference to the original papers.

Conventional photoemission measurements are of two kinds. The spectral yield $Y(h\nu)$ measures the number of emitted electrons per incident photon as a function of photon energy. Energy distributions specify the final energy states of electrons excited by a fixed photon energy. An increase in the yield indicates strong transitions to final energy states from which the electrons can escape into vacuum; a decrease can indicate strong

[1] F. G. Allen and G. W. Gobeli, Phys. Rev. **144**, 558 (1966).
[2] F. G. Allen and G. W. Gobeli, J. Appl. Phys. **35**, 597 (1964).
[3] G. W. Gobeli and F. G. Allen, Phys. Rev. **127**, 141 (1962).
[4] G. W. Gobeli and F. G. Allen, Phys. Rev. **127**, 150 (1922).
[5] G. W. Gobeli, F. G. Allen, and E. O. Kane, Phys. Rev. Letters **12**, 94 (1964).
[6] W. E. Spicer and R. E. Simon, Phys. Rev. Letters **9**, 135 (1962).
[7] J. van Laar and J. J. Scheer, Phillips Res. Rept. **17**, 101 (1922).
[8] M. L. Cohen and J. C. Phillips, Phys. Rev. **139**, A912 (1965).
[9] D. Brust, M. L. Cohen, and J. C. Phillips, Phys. Rev. Letters **9**, 389 (1962).
[10] E. O. Kane, Phys. Rev. **127**, 131 (1962).
[11] E. O. Kane, J. Phys. Soc. Japan **21**, Suppl. 37 (1966).
[12] W. E. Spicer and R. C. Eden, Bull. Am. Phys. Soc. **10**, 1198 (1965).
[13] H. R. Philipp and H. Ehrenreich, Phys. Rev. **129**, 1550 (1963).

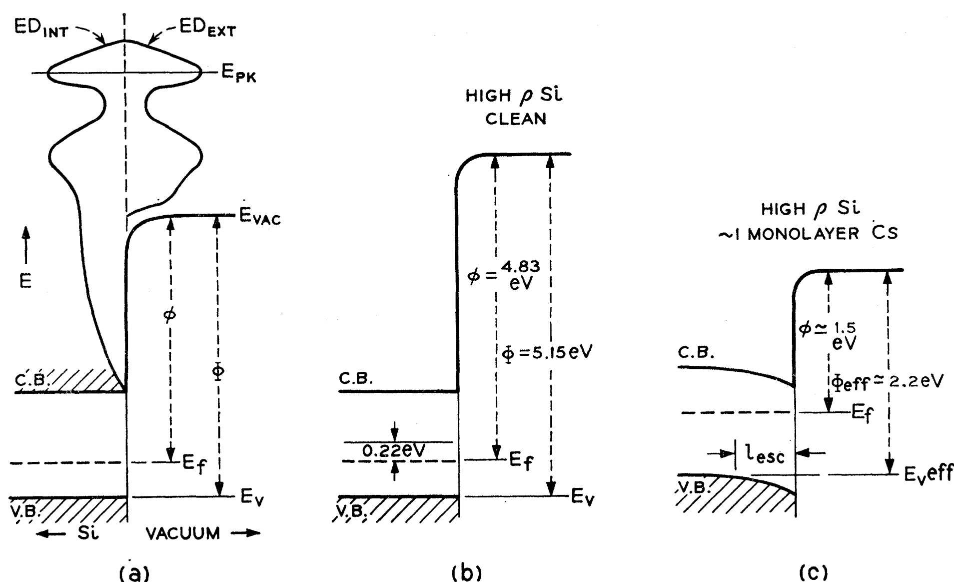

FIG. 1. Energy-level diagrams. (a) Diagram defining parameters useful for interpreting photoemission data; (b) and (c), values of work function φ and photothreshold Φ for clean and cesiated silicon surfaces.

transitions to final states with less than the required escape energy. Structure in the energy distributions give much more detailed information about the electrons which escape by directly measuring their final energy.

The major parameters used to describe photoemission results are given in Fig. 1(a). φ, the work function, is the energy difference between the Fermi level in the crystal and the zero kinetic energy state of an electron in vacuum outside the crystal (henceforth called the vacuum level). Φ, the photoelectric threshold, is the energy difference between the highest filled electron state and the vacuum level. For our purposes, the highest filled state is the top of the valence band, since in lightly doped silicon, photoemission from surface states or bulk states in or above the energy gap are negligible for clean-cleaved silicon and small for cesium covered silicon.[1]

Monochromatic light produces an internal energy distribution of electrons $\mathrm{ED}_{\mathrm{int}}$ as indicated schematically in Fig. 1(a). Structure in this distribution, e.g., the peak E_{pk}, is fixed in energy position with respect to the band structure. Assuming photoexcited electrons suffer predictable energy losses on the way to the surface, each energy position in the external distribution $\mathrm{ED}_{\mathrm{ext}}$ may be associated with the final energy state of an optical transition. To obtain information on band structure, we wish to locate structure in the $\mathrm{ED}_{\mathrm{ext}}$ on this energy scale fixed with respect to the band structure. The retarding potential analyzer, however, measures energy on a scale fixed with respect to the Fermi energy E_f, which varies over the bandgap depending on the nature of the sample and its surface.

In principle, the desired energy scale may be determined by setting the lower edge of the external distribution at the photothreshold Φ, determined by studying the yield near threshold, or by setting the upper limit of the distribution at an energy $h\nu$ above the highest filled state at E_v. Uncertainties in the shape of the escape function and experimental distortions usually make it impractical to determine the energy scale by the method depending on accurate location of the low-energy edge of the distribution. The location of both edges depends on reliably detecting electrons produced by relatively inefficient indirect excitations from a low density of states near the valence-band edge. An alternative method is to measure the work function of sample and collector by an independent method (Kelvin contact-potential measurement), thus determining a scale with respect to the Fermi level. The position of the Fermi level is then determined from the relation $E_f - E_v = \Phi - \varphi$. This method was used by Gobeli and Allen, whose results we use to establish the energy scale in this paper.[1]

A further complication arises when the bands are not flat as in Fig. 1(a), but have slope within the escape depth of the photoexcited electrons as in Fig. 1(c). Then structure in the measured distributions loses resolution by the amount of band bending within the escape depth, and this structure, and the effective photothreshold Φ_{eff}, is measured from some average position of the valence band. Band bending occurs when the Fermi level is pinned by surface states to a different position at the surface of the sample than in the bulk. The transition from surface to bulk values occurs over distances of the order of the Debye length L_D, the screening length for electrostatic charge by free carriers in the sample. In lightly doped silicon ($\rho \gtrsim 10\Omega$ cm) the escape depth $l_{\mathrm{esc}} \ll L_D$, and little curvature occurs within the escape distance so that the surface position of the Fermi level is relevant to the photoemission data. For highly degenerate material where $l_{\mathrm{esc}} \gg L_D$, the bulk value of the Fermi level is the relevant value.

The p-silicon samples used in these experiments have resistivities of 25 and 250Ω cm and calculated bulk Debye lengths of 1200 and 3800 Å, respectively.[14] Since typical escape depths are $\lesssim 100$ Å, the case $l_{\text{esc}} \ll L_D$ applies and the appropriate Fermi level position is nearly that of the surface. Gobeli and Allen have placed the surface Fermi level on a clean-cleaved silicon surface at 0.22 eV below midgap, which is within 0.1 eV of the bulk position of the samples used here.[4] This and the small amount of band bending expected provide nearly perfect flat band conditions within the $\sim$0.1 eV resolution of the photoemission measurements, as is indicated in Fig. 1(b).

The deposition of cesium on a clean silicon surface has two effects. It lowers the work function to about 1.5 eV and shifts the surface Fermi level from below midgap toward the conduction-band edge. Gobeli and Allen suggest that it is moved to the band edge,[1] but our data indicate a position some 0.3 eV below the band edge for full monolayer coverage. Assuming band bending within the escape depth of about 0.15 eV, an effective threshold of about 2.2 eV is obtained for the fully cesiated surface, as is indicated in Fig. 1(c). Since the collector measures energy with respect to the Fermi level, lowering the work function allows lower energy portions of the internal electron distribution to escape. The shift of the surface Fermi level shifts all observed structure on the measured energy scale by an amount equal to the Fermi level shift minus the band bending at some average escape depth of the electron. Both effects of depositing cesium will be clearly seen in the data.

Photoemitted electrons have been acted upon by three processes. Photoexcitation from the valence band to the conduction band produces an initial internal energy distribution. Transport processes can modify the distribution between the point of excitation and the surface. Finally, the electrons are transmitted through the surface into the vacuum. These three processes will be considered briefly in order.

Several workers have interpreted photoemission data from silicon assuming direct optical transitions, i.e., assuming transitions between one-electron states in which crystal momentum is conserved.[8–10] According to this theory, structure in the spectral yield is expected at critical points in the joint density of states when $\nabla_k[E_n(\mathbf{k})-E_p(\mathbf{k})]=0$, where E_n and E_p are electron states in the conduction band and valence band, respectively. At points in k space of high crystal symmetry (Γ,L), the stronger condition $\nabla_k E_n(\mathbf{k})=\nabla_k E_p(\mathbf{k})=0$ holds. An early hope of photoemission experiments was that the energy position of such high-symmetry points could be experimentally determined from photoemission measurements. Kane's calculations for silicon for photon energies <6.2 eV indicate that clusters of general critical points lie near in energy to the high-symmetry critical points and effectively mask their contribution to the initial energy distributions.[15] This result, and transport effects to be discussed below, has prevented the positive identification of high-symmetry points in silicon on the basis of previously published photoemission data.

The three-dimensional critical point theory outlined above applies directly only to structure in the yield or in optical absorption. Kane has developed the related theory necessary for interpreting structure in the internal energy distributions.[16] He computes the density of states satisfying the conditions $E_n(\mathbf{k})-E_p(\mathbf{k})=h\nu$, and $E_n(\mathbf{k})=E$, where E is an energy position in the internal distribution. Points where the surfaces defined by these two expressions are tangent are two-dimensional critical points that will produce structure in the distributions. At two-dimensional critical points where the surfaces cross (saddle points), a peak appears in the theoretical distribution. At points where the surfaces just touch but do not cross (extremal points), a discontinuous change in the joint density of states common to both surfaces produces a shoulder in the distribution. As $h\nu$ is varied, two-dimensional critical points move on trajectories in k space called critical lines. These lines in k space have an image on a plot of energy position of structure versus photon energy that may be compared directly with experimental plots of structural position versus photon energy such as is given in Fig. 6. Each three-dimensional critical point defined in the previous paragraph has one or more critical lines passing through it. At values of photon energy where two-dimensional and three-dimensional critical points coincide, the structure in the distribution associated with the two dimensional critical point will be enhanced.

Spicer and co-workers have noted that in many materials other than silicon, peaks in the external energy distributions are either stationary or move in energy position by an amount exactly equal to the change in the photon energy.[17] They interpret both types of structure in terms of nondirect optical transitions. These are defined as transitions whose transition probabilities are proportional to $\rho_c(E)$, the conduction-band density of states at E, multiplied by $\rho_v(E-h\nu)$, the valence-band density of states at $E-h\nu$. Structure in $\rho_c(E)$ produces stationary structure in the excited electron distributions, and structure in $\rho_v(E-h\nu)$ produces the moving structure. Defined in this way, nondirect transitions include (1) direct transitions from (or to) a flat band for which $E(\mathbf{k})$ is constant within the resolution of the experimental data, (2) ordinary phonon assisted indirect transitions, and (3) other transitions that experiments indicate do not conserve crystal momentum, but to which neither of the above categories applies. It is suggested that in some cases this third category of transitions cannot be explained in a way

[14] C. E. Young, J. Appl. Phys. **32**, 329 (1961).

[15] E. O. Kane, Phys. Rev. **146**, 558 (1966).

[16] E. O. Kane (unpublished); a summary is found in D. Brust, Phys. Rev. **139**, A489 (1965).

[17] W. E. Spicer, Phys. Rev. Letters **11**, 243 (1963).

consistent with the normal application of band theory.[18] A crucial point of the nondirect transition theory is that the resulting structure must be either stationary or move at exactly the same rate as the photon energy except of course where the two types of structure overlap for a limited range of photon energies or are modified by transport to and escape through the surface. Other behavior of structure in the external energy distributions weighs heavily against an interpretation in terms of nondirect transitions. The peaks observed in distributions from silicon at photon energies below 6 eV are stationary and therefore are of the type that may be associated with peaks in the conduction-band density of states.

Kane has treated the effects of transport properties on photoelectric measurements.[11,19,20] He finds that phonon scattering, pair-production scattering (an electron-electron collision exciting an additional valence-band electron), and group velocity effects modify the initial distribution. Pair-production scattering results in an average energy loss of several eV per collision. It distorts the distributions by deleting high-energy electrons and superposing a secondary distribution on the lower energy portion of the primary distribution. Structure in this secondary distribution strongly reflects structure in the ordinary conduction-band density of states.[11,20]

The mean free path for phonon scattering $l_{\rm ph}$ is related to the phonon scattering rate $1/\tau_{\rm ph}$ by the group velocity v_g;

$$l_{\rm ph}=v_g\tau_{\rm ph}.$$

Both v_g and $\tau_{\rm ph}$ vary approximately inversely with $\rho_c(E)$, the conduction-band density of states. At electron energies where phonon scattering is important, the escape probability at a given energy of the internal electron distribution varies approximately as $l_{\rm ph}$. Increased scattering at high state densities results in a larger average energy loss and a decreased escape probability. Thus, when phonon scattering dominates the energy-loss mechanism, a peak in the density of states may result in a dip in the external distribution with a peak, or excess of degraded electrons at immediately lower energy.

Kane has invoked this effect to account for the peak and dip observed at $E_v+3.8$ eV and $E_v+4.1$ eV, respectively, in the silicon distributions. (See Fig. 5, peak No. 2.[11]) Present calculations show a high state density at about this energy, but do not locate it unambiguously enough to resolve the question of whether the high density of states is at the position of the peak as suggested by Spicer,[21] or of the dip at slightly higher energy as suggested by Kane.

Electrons that reach the surface may be reflected back into the crystal or transmitted into the vacuum with a fixed constant energy loss equal to the energy of the vacuum level. For clean, ordered surfaces, many electrons pass through the surface unscattered.[5] For cesium coated surfaces, momentum is randomized in passing through the surface. If we assume here that energy losses in this scattering are small, the effect of the surface can be specified in terms of a transmission coefficient. The calculation of a transmission coefficient is difficult and questionable at best, as are most calculations for a real surface. The interpretation of the data given below assumes that structure in the external electron distributions more than 0.5 eV above the vacuum level is not attributed to surface effects. An escape-cone factor must always be included in the calculation of the transmission coefficient. Electrons must have sufficient energy *normal* to the surface to surmount the surface barrier. This factor discriminates most strongly against electrons near threshold.

III. EXPERIMENTAL EQUIPMENT

The experimental chamber and vacuum system have been described elsewhere in some detail.[1] The glass vacuum system is pumped with a mercury diffusion pump and trapped with liquid nitrogen. After bakeout it reaches pressures of less than 10^{-10} Torr when undisturbed. Operation of hot filaments and mechanical manipulators during experiments normally increases the working pressure to 1 to 2×10^{-10} Torr. Many features of the multiarmed experimental chamber were unchanged. Among these were the cleavage mechanism, the sample-handling mechanism that allows repeated cleavages on the same sample and experiments on several samples without opening the system to atmosphere, the vibrating molybdenum probe used for measuring work functions by the Kelvin contact potential method, the gold plated retarding potential cage, and the single crystal tungsten ribbon used as a standard when determining the work function.

Two modifications were made in the system. The quartz window of the optical port was replaced by a cleaved LiF window. This window was attached with AgCl to the feathered edge of a silver tube which was brazed to a standard stainless steel to glass seal. When carefully protected from moisture during processing, such a window will transmit to photon energies of about 11.5 eV. The molecular-beam-cesium gun was replaced by a cesium-ion gun consisting of a tungsten filament coated with a zeolite containing cesium. This ion source was developed by workers at the University of Minnesota.[22] Mass spectrograph measurements indicate that the major contaminant ions produced during operation of the gun as percentages of the cesium ions produced are rubidium $\sim1\%$, sodium $\sim\frac{1}{2}\%$, and potassium $<\frac{1}{2}\%$.[23] A pressure burst of CO and CO_2 is observed on

[18] W. E. Spicer, Phys. Letters **20**, 325 (1966).
[19] E. O. Kane, Phys. Rev. **147**, 335 (1966).
[20] E. O. Kane, Phys. Rev. **159**, 624 (1967).
[21] W. E. Spicer, J. Phys. Soc. Japan **21**, Suppl. 42 (1966).
[22] R. E. Weber and L. F. Cordes, Rev. Sci. Instr. **37**, 112 (1966).
[23] J. R. Arthur (private communication).

initial heating of the gun as background gases soaked up from the tube atmosphere are driven off. This burst can be restricted to a duration of a few seconds at pressures of less than 5×10^{-10} Torr by maintaining the gun filament at about 300°K during the cool down from the 250°K bakeout.

Light was supplied for the experiments by a Jarrall-Ash 0.5-m vacuum monochrometer with an Ebert mounting. The 1200 groove/mm replica grating has a reciprocal linear dispersion at the exit slit of 16 Å/mm. Mirror and grating surfaces of evaporated aluminum protected by a film of MgF are designed to provide high and reasonably constant reflectance to beyond the cutoff of the LiF windows used in the experiment.

A Hinteregger-type light source similar to that manufactured by the MacPherson Company was powered by a MacPherson model 720 power supply which may be operated in either a 60 Hz ac mode or to about 1 kHz in a spark discharge mode. Normally, for these experiments, the lamp was operated at hydrogen pressures of 2 to 5 Torr with about 50 mA of line frequency current. Occasionally, a dc power supply providing a maximum current of 300 mA was used when increased light output was required. A LiF window, located between the lamp and the monochrometer, places the major limitation on the short-wavelength range of the system, since this window rapidly solarizes and ceases to transmit wavelengths below about 1260 Å (9.85 eV). Problems with slower solarization at longer wavelengths were adequately solved by using a 1-in. window placed off center at the lamp-output aperture. This window can be rotated to expose four to six clear sections before replacement is necessary.

The output optics of the monochrometer consists of a toroidal mirror, aluminized and coated with MgF, that refocuses the output slit of the monochrometer at a right angle to the output axis of the monochrometer. The crystal surface of interest is placed at this focus so that the area illuminated is equal in size and shape to that of the monochrometer output slit. The monochrometer is attached to the sample chamber by waxing a close fitting metal collar to the optical port of the experimental chamber. The toroidal mirror mount may be moved by external controls about both its vertical and horizontal axis in order to move the light spot over the sample surface.

The light intensity is monitored continually by picking off a portion of the light with a very small aluminized and MgF-coated mirror and deflecting it to a sodium salicylate phosphor. The blue fluorescence from the phosphor was filtered to remove wavelengths shorter than 3600 Å and was monitored by a 6810A RCA phototube. The problem of obtaining a good calibration of the light intensity was not solved at the time of these experiments. The convenient and sensitive phosphor-plus-phototube arrangement has proven to be virtually impossible to calibrate. Sodium salicylate's response is not flat as has often been assumed, nor is it stable with time and exposure to various atmospheres. The latter fact renders even a careful calibration useless in view of the elaborate and time-consuming procedures necessary for making a good calibration at the low light intensities available. Intercomparison of data from various materials is equally uncertain due to the phosphor instability, though Spicer and his students have used this method with some success after careful studies of phosphor response indicated that sodium salicylate films, freshly prepared under carefully controlled conditions, have reproducible structure.[24] For lack of accurate photon-intensity measurements, no detailed yield data will be given in this paper. It is hoped that a Cs_3Sb diode with a LiF or MgF window will provide a suitably stable standard for future work.

The electronics used have been described previously.[1] Briefly, a Cary electrometer is used to measure the number of photoemitted electrons which reach a retarding potential cage. An accurate voltage ramp, produced by electronically integrating a battery voltage, is applied between cage and sample surface to drive the photocurrent from saturation to cutoff. The signal from the electrometer is electronically differentiated and plotted versus the ramp voltage on a Moseley X-Y recorder. The plotted curves are the electron energy distributions modified by distorting factors inherent in the experimental technique. These are described below. The minimum photoemission currents necessary to obtain usable distribution curves varies from 1 to 5×10^{-13} A, depending on the energy width of the distribution. At current levels above about 10^{-12} A, structure can be much more reliably resolved. In order to obtain reasonably noise-free distributions at these low current levels, it is necessary to completely shield the sample chamber and electrometer head and to filter frequencies higher than 6 cps before the electronic differentiation.

Several major factors distort the measured distributions. They are the energy spread of light from the monochromator, distorted retarding fields due to imperfect cage geometry, fringing fields due to work function differences between the emitting surface and other surfaces of the sample, patch effects due to uneven work functions of the sample or collector surface, and field gradients within the escape depth of the photoexcited electrons that distort the energy bands inside the sample surface.

One-mm slits were used in these experiments. The 16 Å/mm reciprocal dispersion at the output slits then gives a photon energy spread of 0.045 eV at 6 eV (2070 Å) and 0.12 eV at 10 eV (1240 Å). The smearing of the distribution due to cage geometry is very difficult to calculate for the cylindrical geometry of the collector. From experimental evidence, Gobeli and Allen estimate it to be $\lesssim$0.15 eV. They estimate also that smearing of the distributions due to variations in the work function of the collector are $\lesssim$0.1 eV.[1] Nonuniform emitter

[24] R. Koyama and W. E. Spicer (private communication).

potential and fringe fields have the same effect of drastically smearing the low-energy edge of the distributions. Electrons with low kinetic energy emitted toward such a field cannot surmount it until very large voltages are applied to the distant collector, while electrons with energies sufficient to penetrate the fringe field reach the collector with no degradation of their energy. As might be expected, these effects are very strong for the cesiated surfaces, extending their low-energy tails by more than a volt; on clean-cleaved surfaces the effects are small. The high-energy portion of all distributions should be unaffected, however. We have seen above that band-bending effects are negligible for the clean surfaces and provide a maximum smearing of ~0.15 eV for the cesium-covered surface. Except at the low-energy end of the distributions, then, the over-all resolution for the clean surface varies from about 0.15 eV at photon energies of 6 eV to about 0.25 eV at photon energies of 10 eV. Resolution for the cesiated surface is somewhat worse.

Details of the preparation of samples, the cleavage technique, and the nature of the resulting surfaces have been discussed in detail elsewhere.[25] Typically, an area of 1mm×7mm of a total sample surface area of 2 mm×10 mm will show good cleavage. In these experiments, light was focused on the sample in a spot of dimensions 1 mm×5 mm. Inevitably, a small part of the photoemission came from fractured surface near the well-cleaved area. No improvement in resolution or significant change in shape of the distributions accompanied the use of a smaller spot size, however, so the larger spot size was used to gain maximum photocurrent output.

IV. EXPERIMENTAL RESULTS AND DISCUSSION

The data presented in this section were taken from two samples of boron-doped *p* silicon. Surfaces 4-0 and 6-0 refer to clean-cleaved (111) faces of a 25 and a 250Ω cm sample, respectively. Surfaces 6-1 through 6-5 refer to the face of the 250Ω cm sample after each of five successive cesium depositions.

A. Effect of Cesium Deposition

Figure 2 shows the effect of cesium deposition on a distribution taken at $h\nu=7.85$ eV. The areas under the curves are adjusted to total yield. Calculated coverages are shown in terms of monolayers where one monlayer is taken equal to 8×10^{14} ion/cm^2, the approximate number of surface sites on a (111) silicon surface. We recall that on the retarding potential scale, a shift in the lower edge of the distributions indicates a change in work function and that a shift of structure or of the upper edge of the distributions indicates shift of surface Fermi level with respect to the energy-band structure, as

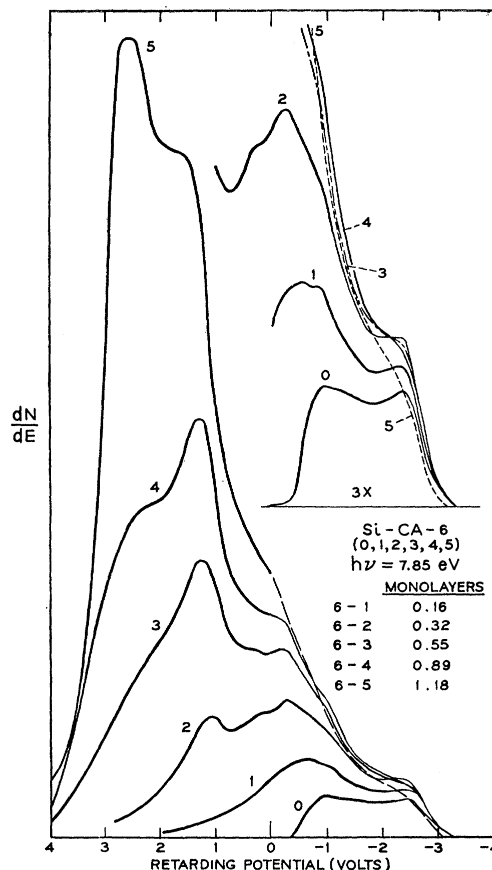

FIG. 2. Effect of cesium deposition on a clean silicon surface.

modified by band bending. Using these criteria, the work functions is clearly reduced at each successive coverage, the total reduction observed after coverage 5 being about 3.5 eV. This is the maximum reduction found at full monolayer coverage in previous work. Long low-energy tails on the distributions taken at intermediate coverages show the effects of fringe fields and uneven cesium deposition. This low-energy tail is much reduced near full coverage. These changes in work function were confirmed by Kelvin contact-potential measurements.

The increase of emission at the upper edge of the distributions after depositions 1 and 2 probably reflects the opening up of the escape cone. The high-energy limits and shoulder of these distributions show no change in position or loss of resolution that would indicate a shift of the surface Fermi level. Resolution of the upper edge and other structure is progressively reduced in depositions 3–5. The energy positions of structural features are estimated to shift by 0.1 eV after deposition 4 and by 0.25 after 5. These shifts were estimated by comparing plotted energy positions of all structure in all the distributions taken after each deposition. The shifts in the upper limits of distributions from 6-4 and 6-5 are less than 0.1 eV and 0.25 eV, respectively, probably

[25] G. W. Gobeli and F. G. Allen, J. Phys. Chem. Solids 14, 23 (1960).

because this limit is produced by transitions in the deepest emission region having maximum band bending rather than by transitions from the entire escape region having, on the average, less band bending. Allowing for band bending in material of this purity, the maximum shift in surface Fermi level consistent with structural shifts observed is about 0.4 eV. This is much less than the 0.75 eV shift that would be observed if the surface Fermi level moved from a position below midgap on the clean surface to the conduction band on the covered surface as previously reported.

A possible experimental cause for this discrepancy, contamination of the collector cage by cesium, was ruled out by exposing a new cleavage surface which showed structure in the same energy position as surface 6-0. It is probable that the coverages given are overestimates due to some cesium ions being collected on the sides of the sample. This effect cannot exceed 20 or 30% and still give the observed change in work function. There is also doubtless some unevenness in the cesium coverage. Giving full weight to these factors and the limited resolution of the experiments, the following conclusions remain valid. (1) The work-function shift of 3.5 eV indicates full or nearly full monolayer coverage over the sample surface after the fifth cesium deposition. (2) Within experimental resolution of $\sim$0.15 eV, no shift of the surface Fermi level is detected to cesium coverages of approximately $\frac{1}{3}$ monolayer. (3) The maximum shift of the surface Fermi level indicated by the present data for approximately one monolayer cesium coverage is 0.4 eV. Accepting the Fermi level position on the clean surface as being well established at $\sim$0.2 eV below midgap, this indicates a final position of the surface Fermi level some 0.3 eV or more below the conduction-band edge. We note here that the evidence cited by Allen and Gobeli for a final position of the surface Fermi level near the conduction band is not conclusive and appears to be equally consistent with a position deeper in the band gap.

It has been proposed that cesium ions have donor levels at or above the conduction-band edge.[1,26] The charge of the cesium ions is compensated partly by electrons in surface states having empty energy levels in the band gap and partly by electrons in bulk states. The above evidence indicates that most compensating electrons are in surface states since few bulk states are available below the conduction band edge. Moreover, it suggests that a high density of available states near the clean surface Fermi level prevents rapid change of the surface Fermi level in the initial states of cesium deposition. When these states are saturated, higher-energy surface states are filled carrying the Fermi level to a position in the upper half of the band gap. This distribution of surface states is strikingly like that proposed by Gobeli and Allen for clean silicon on the basis of photoelectric threshold and work function measurements.[4] Their data indicate that there are approximately as many surface states as surface atoms and that these states are symmetrically located in two bands $\lesssim$0.15 eV on either side of the clean surface Fermi level. The present results suggest a similar distribution of states for partial cesium coverage in that there must be a large density of empty surface states near the clean surface Fermi level position. We regard the model proposed here to explain the effects of cesium coverage on the photoelectric energy distributions as tentative. Further experiments are planned that may serve to confirm it.

It is not entirely correct that filled surface states serve only to lower the work function. If their wave functions penetrate into the bulk for distances of the order of the average excitation depth of emitted electrons, band bending from this source will effect the distributions. The values of band bending given above were estimated somewhat loosely from the data and are greater than would be calculated assuming negligible penetration of surface states. Such surface-state band bending may be the cause of the discrepancy.

B. Determination of Energy Scale for Distributions

The retarding potential scale is fixed with respect to the Fermi level of the measured surfaces. We have seen above that cesium depositions 4 and 5 shift structure in the distributions by 0.1 and 0.25 eV, respectively. Correcting for these shifts, caused by changes in the relative position of band structure and the Fermi level, we obtain an energy scale fixed with respect to the band structure at the average photoemission depth. If we fix the energy position of a single structural feature of the energy distributions on this scale, the energy position of all structure is fixed with respect to the band structure. In agreement with other authors,[1,6] we assign a value of $E_v+3.8$ eV to peak 2 to obtain the energy scale marked $E-E_v$ in Figs. 3 through 6.

C. Energy Distributions of Photoemitted Electrons

Figures 3(a) and 3(b) show energy distributions of photoemitted electrons taken from the clean silicon surface 4-0 with incident uv irradiation of photon energy 6.74 to 9.63 eV. The distributions are scaled arbitrarily for clarity since good yield data, which would allow scaling areas proportional to the total yield, are not available. The lower scale in these and succeeding curves is the potential applied to the collecting cage. The upper scale is the energy of the emitted electrons above the valence-band edge, determined as explained in Sec. IV B. The approximate position of features of interest are indicated by lightly drawn lines numbered from 7 to 11. All features so marked have been identified and found to be reproducible on several surfaces. In particular, all features indicated are also present on the surface 6-0, to which cesium was later applied. The relative

[26] I. Langmuir, Chem. Rev. 13, 147 (1933).

height of the prominent peak marked 10 was somewhat lower in the distributions from surface 6-0 than in those from 4-0.

Figures 4(a) and 4(b) show distributions taken from the partially cesiates surface 6-2 at photon energies between 5.39 and 9.19 eV. Some structure observed in distributions from the clean surface is still resolved here. In addition the energy position of peaks designated 4, 5, and 6 and the dip designated 3 can be followed as the photon energy is varied. Distributions from other surfaces with cesium coverages less than one monolayer are not published since they do not reveal additional struc-

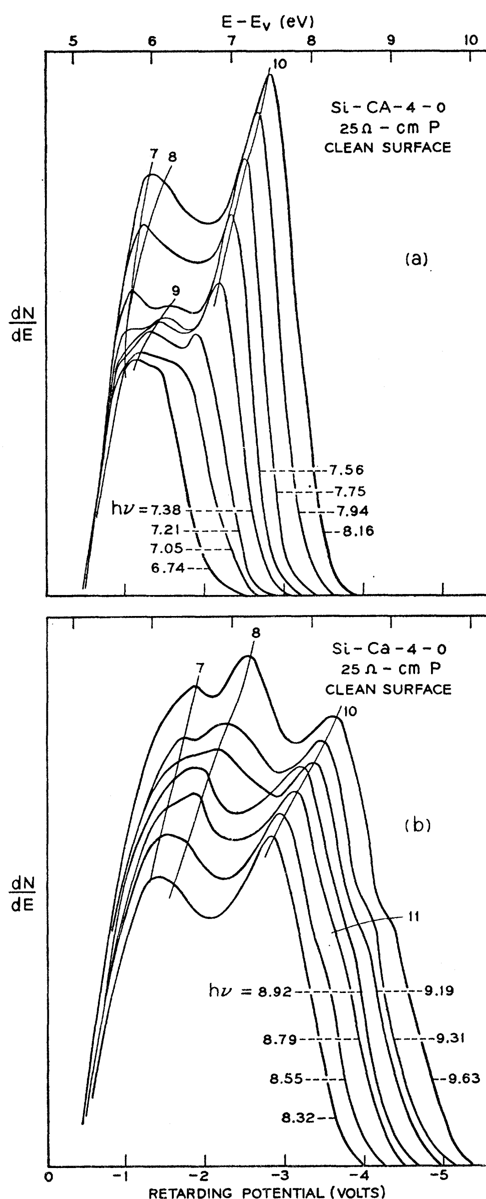

FIG. 3. Energy distribution of photoemitted electrons from a clean silicon surface.

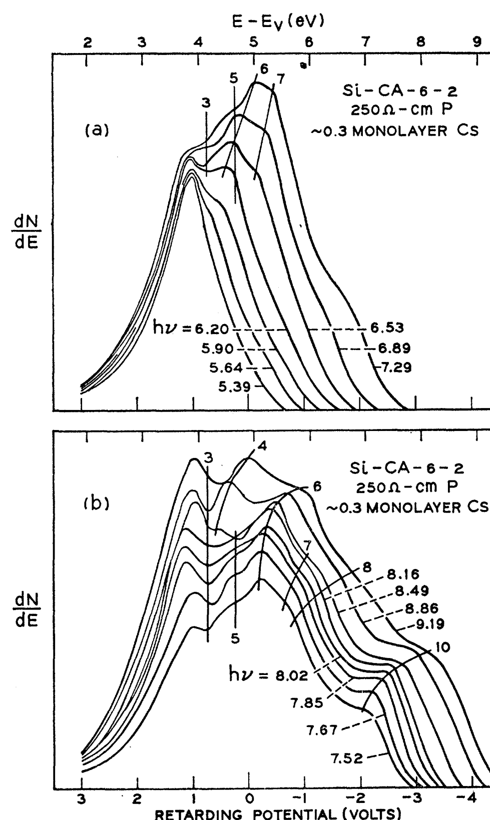

FIG. 4. Energy distributions of photoemitted electrons from a silicon surface with ~0.3 monolayers of cesium.

ture. Note, however, that all structure identified has been observed in distributions from two or more surfaces of different coverage. Figures 5(a) and 5(b) show distributions taken at photon energies between 3.26 and 9.19 eV on a surface with a full monolayer of cesium (surface 6-5). Most structure observed at smaller cesium coverages is broadened and washed out. The distributions are now completely dominated by the two broad low-energy peaks 1 and 2, and the dip 3, previously identified at photon energies below 6.0 eV.

It is evident from a comparison of Figs. 3–5 that structure at higher final-state energies loses definition as cesium is added to the sample surface. One of the sources of this loss of resolution, band bending, has been discussed previously. Disordering of the surface by cesium deposition also contributes to the loss of resolution. It is known that cesium deposited on a cleaved silicon surface usually forms a disordered layer at low coverages.[27] When deposited as ions at ~10 V, the cesium may, in addition, disorder the silicon surface by displacing atoms or penetrating below the surface. A disordered layer is certainly an effective elastic scatterer, but its importance as an inelastic scatterer of

[27] G. W. Gobeli, J. J. Lander, and J. Morrison, J. Appl. Phys. 37, 203 (1966).

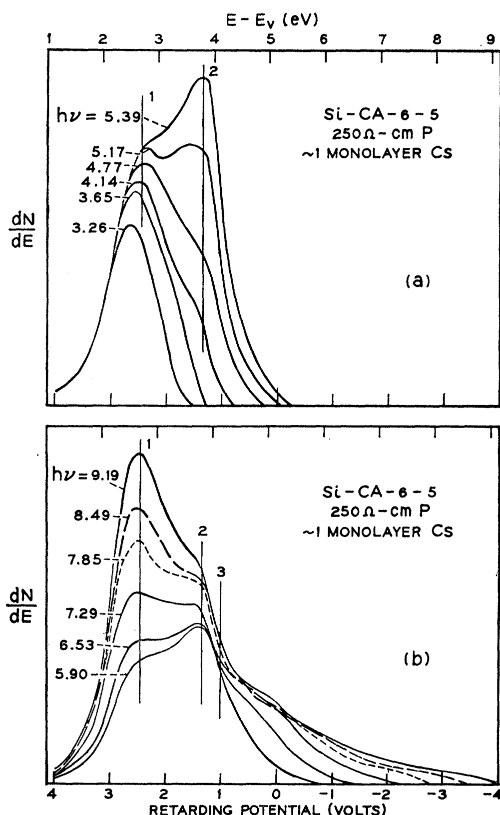

FIG. 5. Energy distributions of photoemitted electrons from a silicon surface with ~1.0 monolayers of cesium.

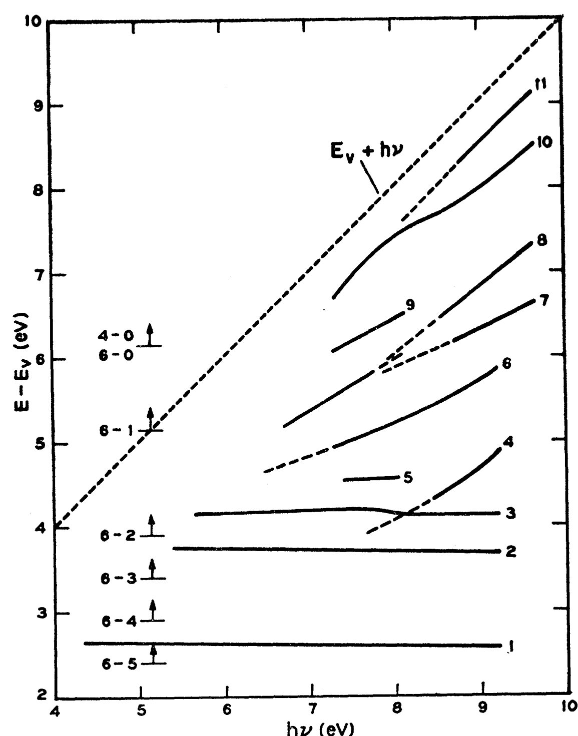

FIG. 6. Energy position of structural features in electron distributions as a function of photon energy.

electrons is not known. Even in the absence of a complete understanding of the effects of cesium deposition, it is clear that the use of fractional monolayers of cesium makes it possible to observe structures that can no longer be resolved at full monolayer coverage.

In Fig. 6 the energy positions of structure in distributions from both clean and cesiated surfaces are plotted as a function of photon energy. Solid lines indicate structure that is clearly resolved and dashed lines indicate the probable position of structure believed to be present, but which is not well resolved. The dotted line marked $E_v+h\nu$ indicates the theoretical upper limit of the distributions for all coverages. The short lines identified by surface designations 4-0, etc., indicate the approximate lower limits of the distributions for cesium coverages 0 through 5. Data from two clean surfaces, 4-0 and 6-0, and from cesiated surfaces 6-1 through 6-5 were plotted to obtain this figure. Only distributions from surface 6-1 added significant information to that obtainable from Figs. 3–5. The location of structure numbered 6 and 7 was aided by data from coverage 6-1.

D. Discussion of Structure

Peaks No. 1 and No. 2 have been previously identified for photon energies $\lesssim 6.2$ eV.[1] These experiments add no new information in that photon energy range. At higher photon energies three features of these peaks are of interest, however. (1) Above 6.2 eV the peaks are stationary in energy within the experimental resolution of the distributions [Figs. 5(b) and 6]. A slight shift (~0.1 eV) toward lower energy as photon energy increases from 6 to 9 eV probably reflects a decrease in average escape depth of the photoemitted electrons (Fig. 6). (2) Peak No. 1 grows rapidly in relative height between 6 and 9 eV [Fig. 5(b)]. Yield data, though of doubtful validity because uncorrected for phosphor response, shows an increase over this photon-energy range. This suggests that the relative size change is associated mostly with the growth of peak No. 1 rather than with the decrease of peak No. 2. (3) Relatively few electrons reach the surface with energies greater than about $E_v+4.5$ eV [Figs. 2 and 5(b)]. We attribute the growth of peak No. 1 and the scarcity of higher energy electrons to the onset of pair-production scattering. Such scattering results in average energy losses of several eV per collision and thus effectively eliminates electrons scattered by this process from the upper 2 or 3 eV of the distributions.

Kane's calculations show that pair production competes with phonon scattering in the electron-energy range from E_v+4 to E_v+7 eV and becomes the dominant scattering process above about E_v+7 eV.[11] The distributions produced by scattering of photoexcited electrons and holes with energies between about E_v+4

eV and E_v+9 eV show a high density of secondaries below a peak at $E_v+2.8$ eV with a rapid decrease in density at higher energies.[20] These calculated results are in excellent agreement with our data.

The dip No. 3 affects the distributions of Fig. 5(b) but cannot be clearly distinguished there. It is clearly evident in Figs. 4(a) and 4(b), however. The dip is a primary feature of the distribution and not just a valley between adjacent peaks. This can be seen in Fig. 4(b) as peak No. 4 passes across the position of the dip. The low-energy shoulder of distributions taken at $h\nu=8.02$ and 8.16 eV is pushed to lower energies as the high density of electrons in peak No. 4 begin to escape. The peak is depressed as it passes under the dip ($h\nu=8.49$ eV) and appears strongly at higher photon energies of 8.86 and 9.19 eV. Shoulder No. 5 appearing intermittently in Figs. 4(a) and 4(b) is thought to be the upper limit of the dip No. 3.

We recall from Sec. II that Kane's calculations indicate a dip at $E_v+4.15$ eV associated with a high density of conduction-band states at that energy. These data strongly confirm the existence of such a dip. Assuming Kane's interpretation is correct, peak No. 2 is at least partially due to electrons initially produced at the energy of the dip and subsequently degraded in energy by transport effects so that they escape at lower energy.

Structural features Nos. 6 through 10 appearing in Figs. 3 and 4 all are peaks that move in energy less rapidly than the change in photon energy. Structure moving with $h\nu$ would have slope equal to that of the line $E_v+h\nu$ in Fig. 6. Consequently, none can be convincingly accounted for in terms of indirect transitions. We believe that they can with assurance be attributed to structure in the joint density of states associated with direct transitions. We consider the abundance of sharp structure apparently associated with direct transitions as distinctly surprising in view of the much more ambiguous situation at lower photon energies and the suggestion that indirect transitions should become increasingly important at higher final-state energies of optically excited electrons. The fact that observed structure is associated with direct transitions does not preclude the possibility that indirect transitions contribute to a relatively structureless background.

Kane has shown that accurate association of structure in energy distributions with band-structure features requires knowledge of direct transition densities throughout the Brillouin zone. Such calculations are available for photon energies $\lesssim 6.2$ eV, but are not yet completed for distributions produced by higher-energy photons. Detailed consideration will be given to the association of distribution structure with band structure when these calculations become available. We hope that it will be possible to associate most of the new structure reported here with the two-dimensional critical points of Kane's theory. The planned theoretical analysis will also include a calculation using a method developed by Bardasis and Hone that allows the effect of both direct and indirect transitions to be included in the same calculation.[28] It is hoped that this will lead to a better understanding of the relative contributions of direct and indirect transitions to the uniform background of our distributions.

The high-energy shoulder of the distributions (peak No. 10 below ~ 8.5 eV and a shoulder No. 11 above ~ 8.7 eV) is most probably the high-energy edge for direct transitions. The distributions extend above this value by more than the instrumental resolution because of the contribution from indirect transitions. The direct transition maxima will occur at the distribution maxima only if there are available states exactly $h\nu$ above the valence-band maxima at the center of the Brillouin zone (Γ point).

V. SUMMARY AND CONCLUSIONS

Measurements of distributions were made on several clean surfaces and on one such surface after each of five successive cesium coverages totaling approximately one monolayer. Data given here from a clean surface, from one surface of intermediate coverage (~ 0.3 monolayer), and from the surface with full monolayer coverage exhibit most of the features that can be traced on the rest of the data.

As cesium is applied to the sample, a shift in the energy of photoemitted electrons relative to the collecting cage at a fixed photon energy reflects a change in the position of the Fermi level at the surface minus the average band bending within the escape depth of the photoexcited electrons. No shift is observed for coverages ≤ 0.3 monolayers and a shift of ~ 0.25 eV is observed at full monolayer coverage. With a generous allowance for band bending, the shift of the surface Fermi level at full coverage is $\lesssim 0.4$ eV. This places the surface Fermi level more than 0.3 eV below the conduction-band edge rather than at the edge as previously reported.[1] The shifts observed as a function of cesium coverage are consistent with a high density of surface states distributed in two bands about the clean surface Fermi level, as proposed by Gobeli and Allen for the clean silicon surface.[4]

Structure appearing in the photoelectron distributions at energy positions less than 4.3 eV above the valence-band edge (E_v) are stationary in energy position at all photon energies in the range $6 \leq h\nu \leq 9.6$ eV. As at lower photon energies, there are two broad peaks centered at $E_v+2.8$ eV and $E_v+3.8$ eV followed by a sharp dip at $E_v+4.1$ eV. The dip is more clearly resolved in our data from the partially cesiated surface than in previously published results from a surface with full monolayer coverage. Its existence tends to confirm Kane's proposal that transport effects are an important factor determining the low-energy structure in the photoemission distributions.

[28] A. Bardasis and D. Hone, Phys. Rev. 153, 849 (1967).

Relatively few electrons reach the surface of the crystal with energies greater than $\sim E_v+4.3$ eV. We attribute this result to the onset of strong pair-production scattering. Secondaries produced by such scattering strongly enhance the peak at $E_v+2.8$ eV at photon energies above 6.5 eV.

A large number of structural features are found at energies in the distributions greater than $E_v+4.3$ eV. This structure changes position with changes in photon energy in a manner that can best be interpreted in terms of direct transitions. This structure will be discussed in detail in a future paper when calculations being undertaken by Brust and Kane become available. These calculations should make it possible to unambiguously associate some of these structural features with details of the band structure.

ACKNOWLEDGMENTS

I wish to thank R. S. Czerwinski for technical assistance, G. W. Gobeli for the loan of much of the equipment used for these measurements, G. W. Gobeli, E. O. Kane, T. E. Fischer, and W. E. Spicer for helpful discussions of this work.

PHYSICAL REVIEW VOLUME 161, NUMBER 3 15 SEPTEMBER 1967

Electronic Effects in the Elastic Constants of n-Type Silicon

JOHN J. HALL
IBM Watson Research Center, Yorktown Heights, New York
(Received 24 April 1967)

The temperature dependence of the second-order elastic moduli, and the 25°C third-order elastic constants, are reported for pure silicon and for silicon doped with $\sim 2\times 10^{19}$ (P atoms)/cm^3. Certain combinations of the elastic constants are unaffected by the doping; others show large changes which are interpreted in the light of Keyes's theory of the electronic contribution to the elastic constants. The agreement between theory and experiment is excellent, and permits a thermodynamic determination of the carrier concentration of the doped sample and of the shear deformation potential constant Ξ_u for the silicon conduction band of 8.6 eV at 25°C.

I. INTRODUCTION

SEVERAL years ago, Keyes[1] pointed out that the elastic properties of a many-valleyed semiconductor, such as n-type silicon or germanium, were dependent upon the electron concentration. The strain produced by an acoustic wave or by uniaxial stress may shift the energies of equivalent conduction-band minima, or "valleys," relative to one another through the deformation potential effect.[2] Electrons in valleys whose energies are raised by strain will transfer to lower-energy valleys until equilibrium is re-established, in a time short compared with the period of the ultrasonic waves to be considered in this work. This transfer results in a lower Fermi energy in the strained crystal, and hence a smaller electronic contribution to the crystal free energy. Since the elastic constants are just the strain derivatives of the free energy, Keyes predicted that the addition of electrons through doping would produce measurable changes in the elastic constants.

Indeed, Bruner and Keyes[3] observed a substantial reduction in the shear modulus C_{44} of heavily doped n germanium, relative to pure germanium, over a range of temperatures, which could be qualitatively explained by Keyes's mechanism. Einspruch and Csavinszky[4] extended Keyes's theory to silicon and measured the effect of doping on the shear constant $C'=\frac{1}{2}(C_{11}-C_{12})$ of a number of n-type samples at several temperatures. Subsequently, Hall[5] and Drabble and Fendley[6] reported large doping effects in the third-order elastic constant C_{456} of germanium, which Keyes had also predicted.

Recent advances in the measurement of sound velocities in solids permit the determination of elastic constants with remarkable precision. The present work will study the changes produced in the elastic constants of silicon by n-type doping. Measurements of the ordinary elastic constants and their temperature dependence will be presented for both pure and heavily doped n-type silicon. In addition, room-temperature measurements of the third-order elastic moduli will be presented for both pure and doped specimens. Keyes's theory will be applied to the conduction band of silicon and the electronic contributions to the elastic constants calculated and compared with experiment. A change found in the shear elastic constant C_{44} upon doping,

---

[1] R. W. Keyes, IBM J. Res. Develop. **5**, 266 (1961).
[2] See, for example, C. Herring and E. Vogt, Phys. Rev. **101**, 944 (1956).
[3] L. J. Bruner and R. W. Keyes, Phys. Rev. Letters **7**, 55 (1961).
[4] N. G. Einspruch and P. Csavinszky, Appl. Phys. Letters **2**, 1 (1963).
[5] J. J. Hall, Phys. Rev. **137**, A960 (1965).
[6] J. R. Drabble and J. Fendley, Solid State Commun. **3**, 269 (1965).